Nuclear Mathematical and Computational Sciences: A Century in Review, A Century Anew
Gatlinburg, Tennessee, April 6-11, 2003, on CD-ROM, American Nuclear Society, LaGrange Park, IL (2003)

ASYMPTOTIC ANALYSIS OF THE SPATIAL WEIGHTS OF THE ARBITRARILY HIGH ORDER TRANSPORT METHOD OF THE CHARACTERISTIC TYPE

Mohamed A. Elsawi
SolidWorks Corp.
12121 Wilshire Blvd, Suite 700
Los Angeles, CA 90025
melsawi@solidworks.com

Naeem M. Abdurrahman
Fluor Hanford, PO Box 1000
Richland, WA 99352
naeem_abdurrahman@RL.gov

Yousry Y. Azmy
Penn State University
Dept. of Mechanical & Nuclear Engineering
229 Reber Building
University Park, PA 16802
yya3@psu.edu

ABSTRACT

We perform asymptotic analysis to the spatial weights of the Arbitrarily High Order Transport (AHOT) method that employs the method of characteristics as a means to relate surface and average fluxes of a computational cell in two-dimensional Cartesian geometry. Previously, the spatial weights of the AHOT's final discrete-variable equations have shown some numerical instabilities as the cell optical thickness approaches zero. Our analysis is based on identifying the components of the spatial weights responsible for these instabilities, then expanding them in a truncated power series of the cell optical thickness that causes the instabilities when approaching zero. We then derive the condition necessary to eliminate the singularity as the cell optical thickness approaches zero. We show that the method we adopted for computing the asymptotic spatial weights is very effective in eliminating these instabilities by comparing the asymptotic weights to the full analytic ones.

Key Words: asymptotic analysis, characteristics method, high-order transport, optically thin cells.

1. INTRODUCTION

Neutral particle transport has constituted one of the most difficult problems in most nuclear engineering applications. Any precise description of neutral particle transport must involve treatment of particles in phase space (space, energy, and time) as influenced by interactions with the host medium. Most of the recent research efforts have evolved around issues related to developing efficient numerical solutions of the multidimensional neutral particle transport equation. The performance of numerical methods for solving the transport equation has been a

major issue in recent research due to their heavy demand on computational resources. In virtually all cases, there has been always a trade-off between the solution accuracy and the overall computational cost. In some cases, though, the solution accuracy is more important than the additional computational cost needed to obtain an accurate solution. For those cases, high-order transport methods have evolved to provide such accurate solutions with reasonable additional computational cost.

An Arbitrarily High Order Transport method of the Nodal type (AHOT-N) has been introduced by Azmy [1] in general-dimension Cartesian geometry, and manipulated in a weighted diamond difference form. The final discrete-variable AHOT-N equations are fully specified by one spatial weight per dimension per discrete ordinate, as opposed to many coefficients in other nodal methods. The numerical results he presented for some two-dimensional test problems indicated that a very high order method, order five, for example, was more computationally efficient, in terms of the computer storage and CPU time, in deep penetration problems than first order methods. Shortly after the introduction of the AHOT-N method, Azmy introduced a two-dimensional "characteristic" version of the AHOT method [2] along the same lines as the AHOT-N method. The main difference between the AHOT-N and the AHOT-C methods is that in the latter, the two-dimensional transport equation is locally solved by the method of characteristics to provide the necessary relationship between the in-cell and the surface evaluated moments of the angular fluxes. One of the most interesting features of the AHOT-C method is that the spatial weights are symmetric about the origin in the angular space, which implies that, if the discrete ordinates used in the angular approximation were symmetric about the origin, only one quarter of those coefficients need to be stored.

The AHOT code was developed to implement the Nodal and the Characteristic options. The code is a steady state, fixed external source, multigroup (with isotropic down scattering only) for solving the transport equation in two-dimensional Cartesian geometry.

It was observed in running the Characteristic option in the AHOT code that numerical instabilities occur when very thin cells are used. By generating gray-scale plots of the flux and source multipliers (i.e., the spatial weights), it was shown that these become contaminated with arithmetic imprecision as the cell size approaches zero. Recently, Azmy [3] has performed thin-cell limit analysis to eliminate these imprecision effects from the flux multipliers.

The purpose of this work is to reconsider the spatial weights of the AHOT-C method as the cell size approaches zero. Specifically, we show that the derived asymptotic expressions are much more accurate than the exact expressions in this limit.

The remainder of this paper is organized as follows. In Section 2 we review the derivation of the AHOT method of the characteristic type and derive the full expressions of the spatial weights. In Section 3 we perform asymptotic analysis on the full expressions of the spatial weights and derive alternative expressions that should be used in situations where the cell size approaches zero. Section 4 shows comparisons of the analytical (full) and asymptotic expressions of the spatial weights and establishes the effectiveness of the thin-cell limit analysis performed in Section 3. We then conclude this paper by offering some suggestions and improvements for future work in Section 5.

2. REVIEW OF BASIC EQUATIONS OF THE AHOT-C METHOD

In this section we review the basic equations of the AHOT-C method and define the full, analytic expressions of the flux and source multipliers (weights).

The Characteristic methods are based on the fact that, in Cartesian geometry, the neutron transport equation possesses straight-line curves along which the streaming operator can be written as a total differential in the characteristic length. We consider the following steady state, monoenergetic, discrete-ordinates approximation of the transport equation in two-dimensional Cartesian geometry,

$$\mu^{\ell}\frac{\partial\psi^{\ell}}{\partial x}+\eta^{\ell}\frac{\partial\psi^{\ell}}{\partial y}+\sigma_T\psi^{\ell}=s^{\ell} \tag{1}$$

where l is the discrete direction index, and s^l is the source term which includes scattering and fission sources. The rest of the notation is standard. The main ingredients of the AHOT-C are as follows:

1. Taking the (i,j)-order moments of the transport equation (1). The resulting set of equations relates the surface-evaluated moments to the cell-averaged moments of the angular flux.
2. Solving the transport equation (1) along the characteristic curves penetrating each cell. The resulting set of equations relates the angular flux at any point (x,y) within the cell to any other point (x_o,y_o) on the same characteristic curve, and the volumetric source moments. By a proper choice of the two points mentioned above, one can relate the surface-evaluated fluxes to the source moments.
3. Solving the discrete-variable equations resulting from steps (1) and (2).

Before proceeding with the final equations, we introduce the following definitions. First, we define the surface moments of the angular fluxes as follows:

$$\psi_{x,j}(\pm a)\equiv\frac{1}{2b}\int_{-b}^{+b}dyP_j(y/b)\psi(\pm a,y)\,, \tag{2}$$

$$\psi_{i,y}(\pm b)\equiv\frac{1}{2a}\int_{-a}^{+a}dxP_i(x/a)\psi(x,\pm b)\,, \tag{3}$$

where $P_k(z/c)$ is the k-th order Legendre polynomial, normalized over the interval $[-c,+c]$ according to the relations

$$\int_{-c}^{c}dzP_k(z/c)P_{k'}(z/c)=\left(\frac{2c}{2k+1}\right)\delta_{kk'}\,, \tag{4}$$

where $\delta_{kk'}$ is the Kronecker delta symbol. Second, we define the cell flux and source moments by:

$$\psi_{ij} \equiv \left(\frac{1}{4ab}\right)\int_{-a}^{+a} dx P_i(x/a)\int_{-b}^{+b} dy P_j(y/b)\psi(x,y)\,, \tag{5}$$

$$s_{ij} \equiv \left(\frac{1}{4ab}\right)\int_{-a}^{+a} dx P_i(x/a)\int_{-b}^{+b} dy P_j(y/b)s(x,y)\,. \tag{6}$$

Upon taking the Legendre moments of the transport equation (1), we obtain the first set of the discrete-variable equations,

$$\begin{aligned}&\left(\frac{\mu}{2a}\right)\left[\psi_{x,j}(a)-(-1)^i\psi_{x,j}(-a)-2\sum_{k=O(i)}^{i-1}{}^{*}(2k+1)\psi_{kj}\right]+\\&\left(\frac{\eta}{2b}\right)\left[\psi_{i,y}(b)-(-1)^j\psi_{i,y}(-b)-2\sum_{k=O(j)}^{j-1}{}^{*}(2k+1)\psi_{ik}\right]+\sigma_T\psi_{ij}=s_{ij},0\le i,j\le I\end{aligned}\,, \tag{7}$$

where the asterisk (*) on the summation operator indicates that the summation index is incremented by 2 and $O(i)=mod_2(i+1)$. Next, we solve the transport equation (1) along the characteristic curves given by $t-t_o=(x-x_o)/\mu=(y-y_o)/\eta$, where (x_o,y_o) and (x,y) are any two points located on the characteristic line as shown in Fig. (1).

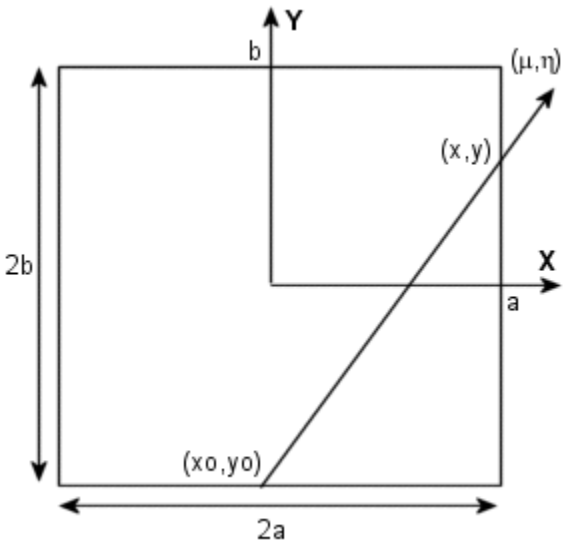

Figure 1. Characteristic curve passing through a computational cell.

On any characteristic curve, the transport equation (1) reduces to,

$$\frac{d\psi}{dt} + \sigma_T \psi = S\,, \tag{8}$$

where *t* is a parameter on the characteristic curve such that $t - t_o$ represents the distance between an arbitrary starting point (x_o, y_o) and the point (x, y) on the same characteristic. Integrating Eq. (8) using an integrating factor yields,

$$\psi(t) = \psi(t_o) e^{-\sigma_T (t - t_o)} + \int_{t_o}^{t} dt' e^{\sigma_T (t' - t)} s(t')\,. \tag{9}$$

The point (x_o, y_o) is usually chosen on one of the cell boundaries where the incoming flux is known, so that $\psi(t_o)$ is known. In order to develop the second set of the discrete-variable equations, we expand the volumetric source in a Legendre expansion, consistent with the moments taken in the derivation of Eq. (6),

$$s(x, y) = \sum_{i,j=0}^{I} (2i+1)(2j+1) s_{ij} P_i(x/a) P_j(y/b)\,. \tag{10}$$

Substituting the parametric equations of the characteristic curve t into the source expansion (10) and inserting the resulting expression into the R.H.S. of Eq. (9) yields,

$$\psi(t) = \psi(t_o) e^{-\sigma_T (t - t_o)} + \sum (2i+1)(2j+1) s_{ij} J_{ij}\ \ , \tag{11}$$

where,

$$J_{ij}(x_o, y_o, t') \equiv \int dt' e^{\sigma_T (t' - t)} P_i\left(\left[x_o + \mu(t' - t_o)\right]/a\right) P_j\left(\left[y_o + \eta(t' - t_o)\right]/b\right). \tag{12}$$

Finally, substituting the equations of the characteristics into Eq. (11) gives,

$$\psi(x, y) = \psi(x_o, y_o) e^{-\sigma_T (x - x_o)/\mu} + \sum_{i,j=0}^{I} (2i+1)(2j+1) s_{ij} J_{ij}\,, \tag{13}$$

$$\psi(x, y) = \psi(x_o, y_o) e^{-\sigma_T (y - y_o)/\eta} + \sum_{i,j=0}^{I} (2i+1)(2j+1) s_{ij} J_{ij}\,. \tag{14}$$

Equations (13) and (14) are equivalent and they represent the relationship between the flux at any point (x, y) within the cell, the flux at any other point (x_o, y_o) on the same characteristic curve, and volumetric source moments. Now we calculate the outgoing flux surface-moments in terms of the incoming flux surface-moments. In order to do so, we evaluate Eq. (13) or Eq. (14)

on the appropriate outgoing surfaces for each member of the set of discrete ordinates, then take the l-th Legendre moment of the resulting expressions along these surfaces. To set the stage for the development of the equations of the AHOT-C method, we consider a rectangular cell of dimensions $2a \times 2b$, which is centered at point $(0,0)$ (see Fig. (2)).

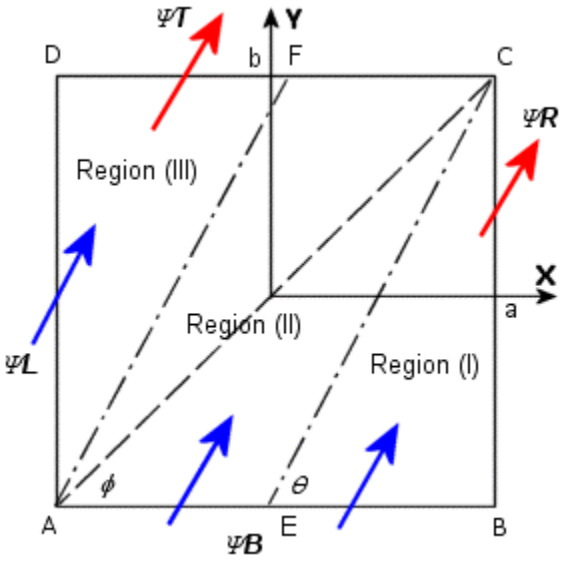

Figure 2. Schematic of a computational cell for the flux moment

The letters L, R, T, and B are used to refer to quantities evaluated at the left, right, top, and bottom faces of the cell. Also, for simplicity, we assume that $\mu,\eta > 0$, that is the neutrons are flowing from left to right and bottom to top. We also introduce the following parameters, $\varepsilon_x \equiv \sigma_T a/\mu$, $\varepsilon_y \equiv \sigma_T b/\eta$, $\theta \equiv \tan^{-1}\left(\frac{\eta}{\mu}\right)$, $\rho \equiv \frac{\eta}{\mu}$, and $\zeta \equiv \tan\theta/\tan\phi = \rho a/b = \varepsilon_x/\varepsilon_y$. Here ε_x, and ε_y are the cell optical thickness in the x and y directions and ζ is a measure of the relative orientation of the cell with respect to the direction of the incident radiation. According to the value of ζ, there are three distinct possibilities: $\zeta > 1$, $\zeta < 1$, and $\zeta = 1$. The difference between these cases is important in determining, for a given direction of radiation incidence, which face will contribute to the outgoing flux. For example, in the case where $\mu,\eta > 0$ and $\zeta > 1$, the incident flux on the bottom face of a cell will contribute to the outgoing fluxes from both the right and top faces of the cell. On the other hand, the incident radiation on the left face will contribute only to the outgoing flux from the top face of the cell. In another case where, for example, $\mu,\eta > 0$ and $\zeta < 1$, the incident flux on the left face of a cell will contribute to the outgoing fluxes from both the right and top faces of the cell. Also the incident flux on the bottom face of the cell will contribute only to the outgoing flux from the right face. Consider for example the case where $\mu,\eta > 0$ and $\zeta > 1$. To identify the contribution of each face to the outgoing flux, we draw a line from the upper right corner of the cell (point C) that is parallel to the direction of incidence of radiation (characterized by μ,η) and intersects the bottom face of the cell at point E (see Fig. (3)). We draw another line from the bottom left corner of the cell (point A) that is parallel to the first line and intersects the top face of the cell at point F. These

two lines divide the cell into three regions (labeled (I), (II), and (III)). In region (I), any radiation enters the cell at the bottom face between points E and B, will contribute to the flux exiting the cell at the right face. In regions (II) and (III), radiation that enters the cell at the bottom face between points A and E, or at the left face will contribute to the exiting flux at the top face of the cell.

In region (I), the incoming flux at the bottom face is given by, $\psi_B(x_o) \equiv \psi(x_o, -b)$ and the outgoing flux is calculated at the right face as $\psi_R(y) \equiv \psi(a, y)$. Taking the l-th Legendre moment of both sides of the above equation by multiplying both sides by $P_l(y/b)/2b$ and integrating over y from $-b$ to $+b$ yields,

$$\psi_{R,l} = \sum_{i=0}^{I} (2i+1) T_{i,l}(\varepsilon_y, \zeta) \psi_{B,i} + \sum_{i,j=0}^{I} (2i+1)(2j+1) s_{ij} S_{ijl}, \tag{15}$$

where the function $T_{i,l}$ is defined as,

$$T_{i,l}(\varepsilon, \zeta) \equiv \frac{e^{-\varepsilon}}{2} \int_{-1}^{+1} dc P_i\left(1 - \frac{1+c}{\zeta}\right) P_l(c) e^{-c\varepsilon}, \tag{16}$$

and S_{ijl} is given by,

$$S_{ijl} = \frac{1}{2b} \int_{-b}^{+b} dy P_l(y/b) J_{ij}(a, y, \tau). \tag{17}$$

Similar calculations are performed to compute the outgoing flux at the top face of the cell. We show the final flux moment equations:

$$\psi_{T,l} = \sum_{i=0}^{I} (2i+1) \left[N_{i,l}(\varepsilon_y, \zeta) \psi_{B,i} + M_{i,l}(\varepsilon_x, \zeta) \psi_{L,i} \right] + \sum_{i,j=0}^{I} (2i+1)(2j+1) s_{ij} R_{ijl}, \tag{18}$$

where the functions $N_{i,l}$, $M_{i,l}$, and R_{ijl} are given by,

$$N_{i,l}(\varepsilon, \zeta) \equiv \frac{e^{-2\varepsilon}}{2} \int_{2/\zeta - 1}^{+1} dc P_i\left(c - \frac{2}{\zeta}\right) P_l(c) \equiv e^{-2\varepsilon} \nu_{i,l}(\zeta), \tag{19}$$

$$M_{i,l}(\varepsilon, \zeta) \equiv \frac{1}{2} \int_{-1}^{2/\zeta - 1} dc P_i(1 - \zeta[1+c]) P_l(c) e^{-\varepsilon(c+1)}, \tag{20}$$

$$R_{ijl} = \frac{1}{2a} \int_{-a}^{+a} dx P_l(x) J_{ij}(x, b, \tau). \tag{21}$$

The discrete-variable equations, Eqs. (7), (15), and (18), and the global boundary conditions are solved via the standard mesh sweeps in each discrete direction. For example, for $\mu,\eta>0$, given $\psi_{l,y}(-b)$ and $\psi_{x,l}(-a)$ from adjacent cells or the global boundary conditions, Eqs. (15) and (18) are solved for $\psi_{x,l}(a)$ and $\psi_{l,y}(b)$, where $l=0,...,I$, then Eq. (7) is solved for ψ_{ij}, where $i,j=0,...,I$. At this point, it is worth mentioning that the practical motivation for developing the AHOT-C method is that higher computational efficiency of high order methods in problems with large homogeneous regions is achievable. Moreover, by using high order methods, consistent interpolation formulae for computing detailed flux distributions within large cells and on surfaces of irregular meshes are obtained, which produce very accurate reference solutions to benchmark problems.

3. ASYMPTOTIC ANALYSIS OF THE SPATIAL WEIGHTS OF THE AHOT-C

It was observed in running the characteristic option in the AHOT code that numerical instabilities occurred when the computational cells are optically thin. Plots of the flux and source multipliers showed that these become contaminated with arithmetic imprecision as the cell size approaches zero. Hence a reconsideration of the spatial weights for the AHOT-C is necessary to remove this undesired behavior.

3.1 Introduction

The term flux multipliers is defined as the spatial weights which multiply the surface flux moments in the final discrete-variable equations of the AHOT-C method. For example, in Eq. (15), the terms $(2i+1)T_{i,l}(\varepsilon_y,\zeta)$ are the flux multipliers in region (I) of a computational cell that multiply the incoming surface flux moments at the bottom face in the case where $\mu,\eta>0$ and $\zeta>1$. Similarly, in Eq. (18), the quantities $(2i+1)N_{i,l}(\varepsilon_y,\zeta)$ and $(2i+1)M_{i,l}(\varepsilon_x,\zeta)$ are the flux multipliers in regions (II) and (III) of a computational cell that multiply the incoming surface flux moments at the bottom and left faces in the case where $\mu,\eta>0$ and $\zeta>1$. We can think of the flux multipliers as a weighting of the contribution of the incoming flux moments to the outgoing flux moments of a cell. In the next section we will define the first, second, and third flux multipliers and review the asymptotic analysis of these coefficients in the limit as the cell optical thickness approaches zero. At this point the asymptotic analysis will be carried out in terms of the variable ε_y, where ε_y refers to the cell optical thickness in Y direction.

3.2 Asymptotic Analysis of Flux Multipliers

This section is devoted to presenting the asymptotic analysis for the three flux multipliers.

3.2.1 First flux multiplier

The first flux multipliers are defined as the flux multipliers in region (I) of a computational cell. Again we define region (I) of a computational cell as that part of the cell for which all characteristic curves drawn parallel to the direction of radiation incidence, and starting from the face where radiation exits the cell, intersect only one face of the cell. In other words, the outgoing flux of this region results from the incoming flux on only one face of the cell. The first flux multipliers can generally be written as $A(2i+1)T_{i,l}(\varepsilon,\zeta)$ where A depends on the moments of the incoming and outgoing fluxes, ε is the cell optical thickness in either X or Y direction, and ζ is the cell aspect ratio. The function $T_{i,l}(\varepsilon,\zeta)$ is defined by,

$$T_{i,l}(\varepsilon,\zeta) \equiv \frac{e^{-\varepsilon}}{2}\int_{-1}^{+1} dc P_i\left(1-\frac{1+c}{\zeta}\right)P_l(c)e^{-c\varepsilon} \ . \tag{16}$$

Integrating the above equation by parts yields,

$$T_{i,l}(\varepsilon,\zeta) = \frac{1}{\varepsilon}\left\{\frac{(-1)^l - e^{-2\varepsilon}P_i(1-2/\zeta)}{2} + \sum_{k=O(l)}^{l-1}{}^{*}(2k+1)T_{i,k}(\varepsilon,\zeta) - \sum_{k=O(i)}^{i-1}{}^{*}(2k+1)T_{k,l}(\varepsilon,\zeta)\right\}, \tag{22}$$

which explodes as $\varepsilon \to 0$, even though Eq. (16) does not explode in this limit. An alternative formula to Eq. (22) is needed that does not involve the reciprocal of ε and allows us to compute $T_{i,l}(\varepsilon,\zeta)$ as $\varepsilon \to 0$ with good precision. Using recursive formulas for Legendre polynomials, the following alternative to Eq. (22) is obtained,

$$T_{i,l}(\varepsilon,\zeta) = \frac{1}{i\zeta}\left[(2i-1)(\zeta-1)T_{i-1,l} - \zeta(i-1)T_{i-2,l} - \frac{(2i-1)(l+1)}{(2l+1)}T_{i-1,l+1} - \frac{l(2i-1)}{(2l+1)}T_{i-1,l-1}\right]. \tag{23}$$

Eq. (23) does not involve the reciprocal of ε and thus will provide a good limit for thin cells. In order for the above recursive formula to work, another formula for $T_{0,l}(\varepsilon,\zeta)$ is needed. To do so, we use Eq. (16) with $i=0$, which upon integration by parts yields,

$$T_{0,l}(\varepsilon,\zeta) = T_{0.l-2}(\varepsilon,\zeta) + \frac{(2l-1)}{\varepsilon}T_{0,l-1}(\varepsilon,\zeta). \tag{24}$$

Clearly, Eq. (24) suffers the same problem as Eq. (22), namely, the $1/\varepsilon$ term. Hence we use Eq. (24) to compute $T_{0,l}(\varepsilon,\zeta)$ only if $\varepsilon \geq \gamma$, where γ is a small number say $\gamma = 10^{-4}$. For $\varepsilon < \gamma$, we use a series expansion of $T_{0,l}$ as follows,

$$T_{0,l}(\varepsilon,\zeta) = \sum_{k=0}^{\infty}\alpha_{k,l}\varepsilon^k \ . \tag{25}$$

When substituting Eq. (25) into Eq. (24) and equating the coefficients of ε^l on both sides we obtain the following relations

$$\alpha_{k,l} = 0, \qquad k < l, \tag{26}$$

$$\alpha_{l,l} = -\frac{\alpha_{l-1,l-1}}{(2l+1)}, \tag{27}$$

$$\alpha_{k,l} = \frac{\alpha_{k-1,l+1} - \alpha_{k-1,l-1}}{(2l+1)}, \qquad k \geq l. \tag{28}$$

To compute all the $\alpha_{k,l}$ using Eq. (27), we loop along the direction of the diagonal $k = l$, starting from *k*=0,1,2,… In each case we must have a value for $\alpha_{k,0}$, which was computed to be,

$$\alpha_{k,0} = \left\{1, -1, \frac{2}{3}, -\frac{1}{3}, \frac{2}{15}, \ldots\right\}. \tag{29}$$

To summarize:

$$T_{0,l}(\varepsilon,\zeta) = \delta_{0,l}, \qquad \text{if } \varepsilon = 0, \tag{30-A}$$

$$T_{0,l}(\varepsilon,\zeta) = \sum_{k=0}^{\infty} \alpha_{k,l}\varepsilon^k, \qquad \text{if } 0 < \varepsilon < \gamma, \tag{30-B}$$

$$T_{0,l}(\varepsilon,\zeta) = T_{0,l-2}(\varepsilon,\zeta) + \left(\frac{2l-1}{\varepsilon}\right) T_{0,l-1}(\varepsilon,\zeta), \qquad \text{if } \varepsilon \geq \gamma, \tag{30-C}$$

where the coefficients $\alpha_{k,l}$ are given by Eq.(26) through Eq. (29) then,

$$T_{i,l}(\varepsilon,\zeta) = \frac{1}{i\zeta}\left[(2i-1)(\zeta-1)T_{i-1,l} - \zeta(i-1)T_{i-2,l} - \frac{(2i-1)(l+1)}{(2l+1)}T_{i-1,l+1} - \frac{l(2i-1)}{(2l+1)}T_{i-1,l-1}\right], \; i>0. \tag{30-D}$$

3.2.2 Second flux multipliers

The second flux multipliers are defined as the flux multipliers in region (II) of a computational cell. Region (II) of a computational cell is defined as that region of the cell that extends between two opposite faces where the flux enters from one face and exits at the other. The second flux multipliers can generally be expressed in terms of the function $N_{i,l}(\varepsilon,\zeta)$. This function is defined as,

$$N_{i,l}(\varepsilon,\zeta) \equiv \frac{e^{-2\varepsilon}}{2} \int_{2/\zeta-1}^{+1} dc P_i\left(c - \frac{2}{\zeta}\right) P_l(c) \equiv e^{-2\varepsilon} \nu_{i,l}(\zeta). \tag{31}$$

We use essentially the same procedure as for $T_{i,l}$. Here we show the final results,

$$\nu_{i,l} = \frac{1}{i}\left[\left(\frac{2i-1}{2l+1}\right)\left\{(l+1)\nu_{i-1,l+1} + l\nu_{i-1,l-1}\right\} - \frac{2(2i-1)}{\zeta}\nu_{i-1,l} - (i-1)\nu_{i-2,l}\right], \qquad i \geq 2, l \geq 1, \tag{32-A}$$

with the following initialization equations,

$$\nu_{0,l}(\zeta) = \frac{1}{2(l+1)}\left[P_{l-1}\left(\frac{2}{\zeta}-1\right) - \left(\frac{2}{\zeta}-1\right)P_l\left(\frac{2}{\zeta}-1\right)\right], \; l \geq 1, \tag{32-B}$$

$$\nu_{1,l}(\zeta) = \frac{1}{(2l+1)}\left[(l+1)\nu_{0,l+1}(\zeta) + l\nu_{0,l-1}(\zeta)\right] - \frac{2}{\zeta}\nu_{0,l}(\zeta), \; l \geq 1, \tag{32-C}$$

$$\nu_{i,0}(\zeta) = \frac{1}{i}\left[(2i-1)\left\{\nu_{i-1,1}(\zeta) - \frac{2}{\zeta}\nu_{i-1,0}(\zeta)\right\} - (i-1)\nu_{i-2,0}(\zeta)\right], \; i \geq 2, \tag{32-D}$$

Even though the function $N_{i,l}$ is not singular near $\varepsilon = 0$, we expand it in power series of ε for later use in the asymptotic analysis of the source multipliers. From Eq. (31) we immediately obtain,

$$N_{i,l}(\varepsilon,\zeta) = \nu_{i,l}(\zeta) \sum_{l=0}^{\infty} \frac{(-2)^l}{l!} \varepsilon^l \; . \tag{33}$$

3.2.3 Third flux multipliers

The third flux multipliers are defined as the flux multipliers in region (III) of a computational cell. The third flux multipliers can generally be expressed in terms of the function $M_{i,l}(\varepsilon,\zeta)$. This function is defined as,

$$M_{i,l}(\varepsilon,\zeta) \equiv \frac{1}{2} \int_{-1}^{2/\zeta-1} P_i(1-\zeta[1+c]) P_l(c) e^{-\varepsilon(1+c)} dc \, . \tag{34}$$

The function $M_{i,l}(\varepsilon,\zeta)$ is related to the function $T_{i,l}(\varepsilon,\zeta)$ by the relation,

$$M_{i,l}(\varepsilon,\zeta) = \frac{(-1)^{i+l} T_{l,i}(\varepsilon/\zeta,\zeta)}{\zeta} \, . \tag{35}$$

As the cell optical thickness ε approaches zero, the function $M_{i,l}(\varepsilon,\zeta)$ will follow the function $T_{i,l}(\varepsilon,\zeta)$ in this limit according to Eq. (35), hence no special treatment is needed for it. However, it is appropriate to perform a separate asymptotic analysis of the function $M_{i,l}(\varepsilon,\zeta)$ as the cell optical thickness approaches zero. We will state here the final results of that analysis, a detailed analysis can be found in [4]. The function $M_{0,l}(z,\zeta)$ is expanded in the following power series of *z*, where *z* represents the cell optical thickness,

$$M_{0,l}(z,\zeta)=\sum_{k=0}^{\infty}\beta_{l,k}z^{k}\ ,\ z\le\gamma\,, \tag{36-A}$$

where the coefficients $\beta_{l,k}$ are given by,

$$\beta_{l,0}(\zeta)=-\frac{\Pi_l(\zeta)}{2(2l+1)},\ l\ge 1\,, \tag{36-B}$$

$$\beta_{l,k}(\zeta)=\frac{1}{(2l+1)}\left[\beta_{l+1,k-1}-\beta_{l-1,k-1}-\frac{(-2/\zeta)^k}{2k!}\Pi_l(2/\zeta-1)\right],\ k\ge 1, l\ge 1\,, \tag{36-C}$$

$$\beta_{0,k}(\zeta)=\frac{(-2)^k}{(k+1)!\zeta^{k+1}},\ k\ge 0\,, \tag{36-D}$$

where $\Pi_l(x)\equiv P_{l-1}(x)-P_{l+1}(x)$, $l\ge 1$.

3.3 Asymptotic Analysis of Source Multipliers

The source multipliers are defined as the quantities that multiply the source moments in the final discrete-variable equations of the AHOT-C method, namely, the quantities $(2i+1)(2j+1)J_{ij}$ in Eq. (12) of Section 2. As we mentioned earlier, in the limit where the cell optical thickness in X and/or Y direction approaches zero, the source multipliers suffer from mathematical imprecision and the overall solution deteriorates. Over the next two sub sections we introduce a new approach for computing the source multipliers and provide asymptotic formulas that are working for both the thick and thin cell cases without loss of accuracy. We will derive the asymptotic formulas for the source multipliers for the case $\mu,\eta>0$ and $\zeta<1$. For the rest of cases of radiation incidence and cell orientation, similar formulas were derived [4] but will not be shown here.

3.3.1 Asymptotic analysis of the first source multipliers

The first source multipliers are those coefficients that multiply the source moments in the final discrete-variable equations in region (I) of a computational cell. To distinguish these multipliers

from those in regions (II) and (III), we will refer to the former by the letter $S_{i,j,k}$ whereas we will use the letter $R_{i,j,k}$ to refer to the latter. In this section we present a new approach for calculating the first source multipliers and derive asymptotic formulas that can be used in the thick and thin cell cases as well. The source multipliers are generally defined in terms of the following integral (Eq. (12), Section 2),

$$J_{i,j}(\tau, x_o, y_o) \equiv \int d\tau' e^{\sigma_T(\tau'-\tau)} P_i([x_o + \mu\tau']/a) P_j([y_o + \mu\tau']/b), \tag{12}$$

where (x_o, y_o) refers to any reference point on the characteristic curve that can be parameterized by: $\tau' - \tau = \frac{x - x_o}{\mu} = \frac{y - y_o}{\eta}$. In these equations, (x, y) refers to any point on the characteristic curve and (μ, η) are the direction cosines of the radiation direction of transfer. Using these equations, the integral $J_{i,j}$ can be written in terms of any combination of three variables from $\tau', x, y, x_o,$ and y_o. In other words, we can carry out our derivation in any set of independent variables and manipulate the resulting final expression to obtain the desired dependence. Hence in what follows, we will not explicitly write the arguments of $J_{i,j}$ but it should be understood that only one set of independent variables is used to carry out the derivation. Before proceeding with the derivation of the asymptotic formulas for the source multipliers, we shall set some notations that will be used frequently. We will use the symbols $\mathrm{X}_i(x)$ and $\mathrm{Y}_j(y)$ to refer to Legendre Polynomials of orders i and j, defined on the intervals $(-a, +a)$ and $(-b, +b)$ respectively. That is,

$$\mathrm{X}_i(x) \equiv P_i(x/a), \tag{37-A}$$

$$\mathrm{Y}_j(y) \equiv P_j(y/b). \tag{37-B}$$

Using the definitions (37-A) and (37-B), the $J_{i,j}$ integrals can be rewritten as,

$$J_{i,j}(\tau, x_o, y_o) = \int_0^{\tau} d\tau' e^{\sigma_T(\tau'-\tau)} \mathrm{X}_i(x_o + \mu\tau') \mathrm{Y}_j(y_o + \eta\tau'). \tag{38}$$

The starting point in the asymptotic analysis is to derive recursive formulas for the $J_{i,j}$ integrals. To do so, we insert the following recursive formula for the normalized Legendre polynomials into Eq. (38),

$$\mathrm{X}_i(\xi) = \frac{1}{i}\left\{(2i-1)\frac{\xi}{a}\mathrm{X}_{i-1}(\xi) - (i-1)\mathrm{X}_{i-2}(\xi)\right\}. \tag{39}$$

Upon using the definition of the integrals $J_{i,j}$ into the resulting equation, we obtain the desired recursive formula,

$$J_{i,j}=\frac{1}{i}\left\{(2i-1)\left(\frac{x_o}{a}-\frac{y_o}{\zeta b}\right)J_{i-1,j}-(i-1)J_{i-2,j}+\frac{(2i-1)}{\zeta(2j+1)}\left[(j+1)J_{i-1,j+1}+jJ_{i-1,j-1}\right]\right\}. \quad (40)$$

Eq. (40) can also be written in terms of (x,y) rather than (x_o,y_o) as follows,

$$J_{i,j}=\frac{1}{i}\left\{(2i-1)\left(\frac{x}{a}-\frac{y}{\zeta b}\right)J_{i-1,j}-(i-1)J_{i-2,j}+\frac{(2i-1)}{\zeta(2j+1)}\left[(j+1)J_{i-1,j+1}+jJ_{i-1,j-1}\right]\right\}. \quad (41)$$

Eqs. (40) and (41) are equivalent in the sense that they are used to calculate $J_{i,j}$ from the same lower order integrals. The only difference is that Eq. (40) is used when the coordinates (x_o, y_o) are known whereas Eq. (41) is used when the coordinates (x, y) are known. Another set of equations equivalent to Eq. (40) and Eq. (41) can be obtained by changing the order in which we substitute Legendre recursive relations into Eq. (12). The resulting equations are:

$$J_{i,j}=\frac{1}{j}\left\{(2j-1)\left(\frac{y_o}{b}-\frac{\zeta x_o}{a}\right)J_{i,j-1}-(j-1)J_{i,j-2}+\frac{\zeta(2j-1)}{(2i+1)}\left[(i+1)J_{i+1}+iJ_{i-1,j-1}\right]\right\}, \quad (42)$$

and,

$$J_{i,j}=\frac{1}{j}\left\{(2j-1)\left(\frac{y}{b}-\frac{\zeta x}{a}\right)J_{i,j-1}-(j-1)J_{i,j-2}+\frac{\zeta(2j-1)}{(2i+1)}\left[(i+1)J_{i+1}+iJ_{i-1,j-1}\right]\right\}. \quad (43)$$

Equations (40) and (42) are mathematically equivalent for i and $j > 0$. Equation (41)[(43)] is used to compute $J_{i,j}$ for $j[i]=0$, respectively to avoid singularity. In what follows, we will use Eqs. (40-43) to derive asymptotic formulas for the source multipliers that can be used in the thick and thin cell cases without loss of accuracy. We will start by calculating the first source multipliers in the case $\mu,\eta>0$ and $\zeta<1$.

For the case under investigation, radiation emerges from the cell at $y=b$, and enters the cell at $x_o=-a$ (see Fig. 3).

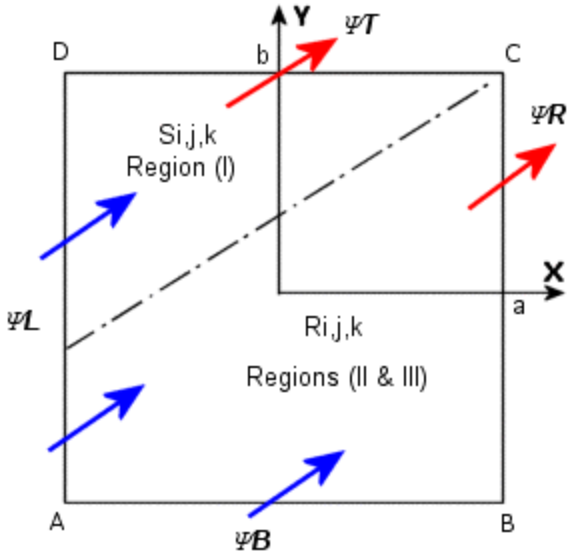

Figure 3. Incoming and outgoing radiation from a 2-D cell for the case $\mu, \eta > 0$ and $\xi < 1$

It follows from Eq. (12) that the first source multipliers are given by,

$$S_{i,j,k} = \left(\frac{1}{2a}\right)\int_{-a}^{+a} \mathrm{X}_k(x) J_{i,j}(x,b,\tau)dx\,. \tag{44}$$

Substituting Eq. (43) into Eq. (44) and manipulating the resulting equation, we obtain the recursive relation for $S_{i,j,k}$,

$$S_{i,j,k} = \frac{1}{j}\left\{ (2j-1)S_{i,j-1,k} - (j-1)S_{i,j-2,k} + \frac{\zeta(2j-1)}{(2i+1)}\left[(i+1)S_{i+1,j-1,k} + iS_{i-1,j-1,k}\right] \right.$$
$$\left. - \frac{\zeta(2j-1)}{(2k+1)}\left[(k+1)S_{i,j-1,k+1} + kS_{i,j-1,k-1}\right] \right\} \quad , \; i \geq 1, j \geq 2, k \geq 1, \tag{45}$$

The recursive formula derived above needs initialization, two levels deep in index *j*, and one level deep in each of *i* and *k* indices. Thus setting *i=0* and *k=0* in Eq. (45) yields,

$$S_{0,j,k} = \frac{1}{j}\left\{(2j-1)S_{0,j-1,k} - (j-1)S_{0j-2,k} + \zeta(2j-1)S_{1,j-1,k} - \frac{\zeta(2j-1)}{(2k+1)}\left[(k+1)S_{0,j-1,k+1} + kS_{0,j-1,k-1}\right]\right\} \tag{46}$$

and,

$$S_{i,j,0} = \frac{1}{j}\left\{(2j-1)S_{i,j-1,0} - (j-1)S_{i,j-2,0} + \frac{\zeta(2j-1)}{(2i+1)}\left[(i+1)S_{i+1,j-1,0} + iS_{i-1,j-1,0}\right] - \zeta(2j-1)S_{i,j-1,1}\right\} \tag{47}$$

Because the R.H.S. of Eqs. (46) and (47) involve only values at *j-1* and *j-2* levels, all *S* quantities are considered known, including those evaluated at *i+1* and *k+1* levels. Next, evaluating Eq. (45) at *j=1* yields,

$$S_{i,1,k} = S_{i,0,k} + \frac{\zeta}{(2i+1)}\left[(i+1)S_{i+1,0,k} + iS_{i-1,0,k}\right] - \frac{\zeta}{(2k+1)}\left[(k+1)S_{i,0,k+1} + kS_{i,0,k-1}\right]. \qquad (48)$$

Now all that remains to make the recursive formulas, i.e., Eqs. (45)-(48), fully functional is to provide an expression for $S_{i,0,k}$. Clearly, Eq. (45) is singular at this value of *j*, so we start with the integral definition of $S_{i,0,k}$, i.e., Eq. (44), which upon using the change of variables yields the following recursive relation for $S_{i,0,k}$,

$$S_{i,0,k} = \frac{1}{\sigma_T}\left[\frac{\delta_{i,k} - \delta_{i-2,k}}{2k+1}\right] - \left(\frac{2i-1}{\varepsilon_x}\right)S_{i-1,0,k} + S_{i-2,0,k}, \qquad i \geq 2, k \geq 0, \qquad (49)$$

with the initialization formulas,

$$S_{1,0,k} = \frac{\delta_{1,k}}{3\sigma_T} + \frac{1}{\sigma_T}T_{0,k}(\varepsilon_x) - \frac{1}{\varepsilon_x}S_{0,0,k}, \qquad k \geq 0, \qquad (50)$$

and,

$$S_{0,0,k} = \frac{\delta_{k,0}}{\sigma_T} - \frac{1}{\sigma_T}T_{0,k}(\varepsilon_x), \quad k \geq 0. \qquad (51)$$

Equations (49)-(51), which are used to evaluate $S_{i,0,k}$ to generate the initialization expressions for $S_{i,j,k}$, in general involve reciprocals of ε_x, and therefore must be analyzed in the limit $\varepsilon_x \to 0$. We start by assuming a series expansion of $S_{i,0,k}$ in the parameter ε_x of the form,

$$S_{i,0,k} = \frac{1}{\sigma_T}\sum_{\ell=0}^{\infty} s_{i,k,\ell}\varepsilon_y^{\ell}, \qquad \zeta\varepsilon_y < \gamma, \qquad (52)$$

where γ is a user defined cutoff value. In the series expansion given by Eq. (52), we used the relation $\varepsilon_x = \zeta\varepsilon_y$ and the cell aspect ratio ζ was absorbed in the expansion coefficients $s_{i,k,l}$. In making this substitution, we assume that the cell aspect ratio is "close" to unity, that is, the cells are not stretched too much in one direction with respect to the other. To calculate the coefficients of expansion in (52), we insert Eq. (52) into Eq. (49) and equate the coefficients of the same power of ε_y on both sides, making sure to set the coefficient of $1/\varepsilon_y$ to zero to avoid singularity as $\varepsilon_y \to 0$, the following set of equations is obtained,

$$s_{i,k,0} = 0,\ k \geq 0, i \geq 1, \tag{53-A}$$

$$s_{i,k,1} = \left(\frac{\zeta}{2i+1}\right)\left[\frac{\delta_{i+1,k} - \delta_{i-1,k}}{2k+1}\right],\ i \geq 1, k \geq 0, \tag{53-B}$$

$$s_{i,k,l} = \left(\frac{\zeta}{2i+1}\right)\left[s_{i-1,k,l-1} - s_{i+1,k,l-1}\right],\ i \geq 1, k \geq 0, l \geq 2, \tag{53-C}$$

$$s_{0,k,l} = \begin{cases} \delta_{0,k} - \alpha_{k,0}, l = 0 \\ -\alpha_{k,l}\zeta^l, l \geq 1 \end{cases}. \tag{53-D}$$

Where $\alpha_{k,l}$ are given by Eqs. (26)-(29). Equations (45)-(53) completely define the calculational procedure for calculating the first source multipliers in the thick as well as the thin cell cases.

3.3.2 Asymptotic analysis of the second source multipliers

The second source multipliers are those coefficients that multiply the source moments in the final discrete-variable equations in regions (II) and (III) of a computational cell. We will refer to those multipliers by $R_{i,j,k}$. As we mentioned earlier, we will limit our analysis of the multipliers to the case $\mu, \eta > 0$ and $\zeta < 1$.

In this case, the outgoing flux is at $x = a$ (see Fig. 3), and the source multipliers in regions (II) and (III) are given by,

$$R_{i,j,k} = \left(\frac{1}{2b}\right)\int_{-b}^{+b} \mathrm{Y}_k(y) J_{i,j}(a, y, \tau) dy. \tag{54}$$

The integrand in Eq. (54) is discontinuous across the characteristic line separating regions (II) and (III). Substituting Eq. (41) for the definition of $J_{i,j}$ into Eq. (54), we obtain the recursive formula for $R_{i,j,k}$,

$$\begin{aligned} R_{i,j,k} = \frac{1}{i}\Bigg\{ & (2i-1)R_{i-1,j,k} - (i-1)R_{i-2,j,k} + \frac{(2i-1)/\zeta}{(2j+1)}\left[(j+1)R_{i-1,j+1,k} + jR_{i-1,j-1,k}\right] \\ & - \frac{(2i-1)/\zeta}{(2k+1)}\left[(k+1)R_{i-1,j,k+1} + kR_{i-1,j,k-1}\right] \Bigg\} \end{aligned}, \tag{55}$$

with the following initialization formulas,

$$R_{i,0,k} = \frac{1}{i}\Bigg\{ (2i-1)R_{i-1,0,k} - (i-1)R_{i-2,0,k} + \frac{(2i-1)}{\zeta}R_{i-1,1,k} - \frac{(2i-1)/\zeta}{(2k+1)}\left[(k+1)R_{i-1,0,k+1} + kR_{i-1,0,k-1}\right]\Bigg\}, \tag{56}$$

$$R_{i,j,0}=\frac{1}{i}\Big\{\ (2i-1)R_{i-1,j,0}-(i-1)R_{i-2,j,0}+\frac{(2i-1)/\zeta}{(2j+1)}\big[(j+1)R_{i-1,j+1,0}+jR_{i-1,j-1,0}\big]-\left(\frac{(2i-1)}{\zeta}\right)R_{i-1,j,1}\Big\},\qquad(57)$$

and,

$$R_{1,j,k}=R_{0,j,k}+\frac{1}{\zeta(2j+1)}\big[(j+1)R_{0,j+1,k}+jR_{0,j-1,k}\big]-\frac{1/\zeta}{(2k+1)}\big[(k+1)R_{0,j,k+1}+kR_{0,j,k-1}\big].\qquad(58)$$

The initialization in the index *i* needs special treatment because Eq. (55) is singular at *i=0*. We use Eq. (54) with *i=0* to obtain, after some algebraic manipulations, the following recursive relation for $R_{0,j,k}$,

$$R_{0,j,k}=\frac{1}{\sigma_T}\left[\frac{\delta_{j,k}-\delta_{j-2,k}}{2k+1}\right]-\frac{1}{\sigma_T}\big[N_{j,k}(\varepsilon_x,1/\zeta)-N_{j-2,k}(\varepsilon_x,1/\zeta)\big]-\left(\frac{2j-1}{\varepsilon_y}\right)R_{0,j-1,k}+R_{0,j-2,k}\quad,\ k\ge 0,\ j\ge 2\,.\qquad(59)$$

The initialization formulas for Eq. (59) are obtained by setting *j=1* and *j=0,* respectively, to obtain the following equations,

$$R_{0,1,k}=\frac{\delta_{1,k}}{3\sigma_T}-\frac{1}{\sigma_T}N_{1,k}(\varepsilon_x,1/\zeta)+\frac{1}{\sigma_T}M_{0,k}(\varepsilon_y,1/\zeta)-\frac{1}{\varepsilon_y}R_{0,0,k}\,,\qquad k\ge 0\,,\qquad(60)$$

$$R_{0,0,k}=\frac{1}{\sigma_T}\big[\delta_{k,0}-M_{0,k}(\varepsilon_y,1/\zeta)-N_{0,k}(\varepsilon_x,1/\zeta)\big],\qquad k\ge 0\,.\qquad(61)$$

Equation (60) involves the reciprocal of the cell optical thickness in the Y direction, which necessitates performing asymptotic analysis for the coefficients $R_{0,j,k}$ in the limit as $\varepsilon_y\to 0$. We begin by assuming a series expansion of the coefficients $R_{0,j,k}$ in powers of ε_y of the form,

$$R_{0,j,k}=\frac{1}{\sigma_T}\sum_{\ell=0}^{\infty}r_{j,k,\ell}\varepsilon_y^{\ell}\,,\qquad \varepsilon_y\le\varepsilon\,.\qquad(62)$$

Substituting the series expansion (62) into Eq. (60) and equating the coefficients of powers of ε_y on both sides, making sure to eliminate the singularity as $\varepsilon_y\to 0$, yields the following equations,

$$r_{j,k,0}=0\,,\qquad j\ge 1\,,\qquad(63\text{-A})$$

$$r_{j,k,1} = \left(\frac{1}{2j+1}\right)\left\{\left[\frac{\delta_{j+1,k} - \delta_{j-1,k}}{2k+1}\right] - \left(\nu_{j+1,k} - \nu_{j-1,k}\right)\right\}, \quad j \geq 1, k \geq 0, \tag{63-B}$$

$$r_{j,k,\ell} = \left(\frac{1}{2j+1}\right)\left\{r_{j-1,k,\ell-1} - r_{j+1,k,\ell-1} - \left(\nu_{j+1,k} - \nu_{j-1,k}\right)\frac{(-2)^{\ell-1}}{(\ell-1)!}\zeta^{\ell-1}\right\}, \ell \geq 2, j \geq 1, k \geq 0, \tag{63-C}$$

$$r_{0,k,l} = \begin{cases} \delta_{k,0} - \nu_{0,k} - \beta_{k,0}, \ell = 0, k \geq 0 \\ -\beta_{k,\ell} - \dfrac{(-2)^{\ell}}{\ell!}\zeta^{\ell}\nu_{0,k}, \ell \geq 1, k \geq 0 \end{cases}. \tag{63-D}$$

Where $\beta_{k,l}$ are given by Eqs. (36-B)-(36-D). The calculational procedure for calculating the second source multipliers is similar to the one used for calculating the first source multipliers in the case $\zeta < 1$.

4. COMPARISON OF THE EXACT AND ASYMPTOTIC FORMULAS

In this section, we compare the exact and asymptotic formulas for the source multipliers we derived earlier in Section 3. We will present the results of our analysis of only those components we identify as the origins of the instabilities in the exact expressions. In producing these results, we have used a symbolic manipulator system that generated the formulas of both the exact and the asymptotic analyses from their analytic representations.

We will start by showing the effect of the asymptotic analysis on the exact expressions of the functions $T_{0,l}$ and $M_{0,l}$. The reason for presenting such results is that these functions are primarily used in evaluating the source multipliers in the original formulation of the AHOT-C method. Fig. 4 shows the exact and asymptotic expressions of the function $T_{0,l}(\varepsilon)$, where ε is the cell optical thickness in either X or Y direction.

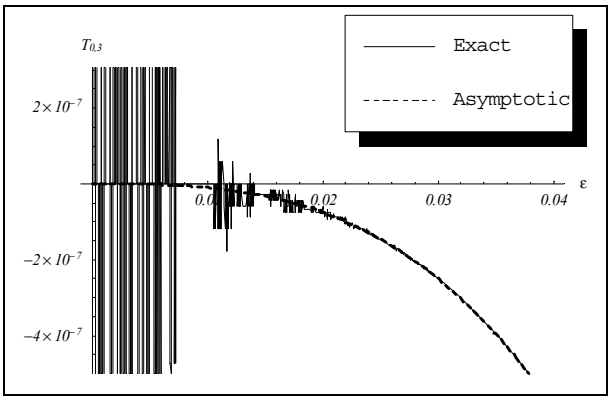

(a)

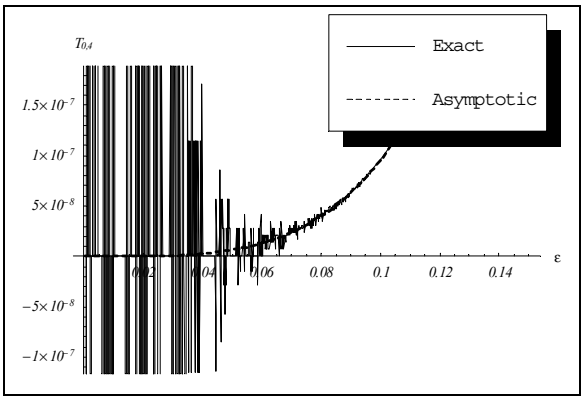

(b)

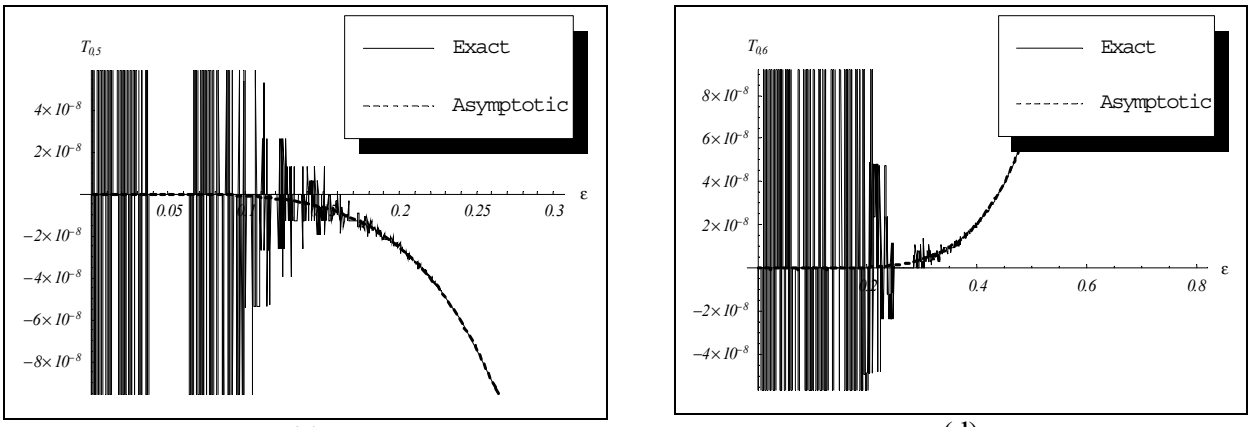

(c) (d)

Figure 4. Exact and asymptotic expressions of the function $T_{0,l}$ of different orders versus the cell optical thickness

We next investigate the function $M_{0,l}$ by plotting its exact and asymptotic expressions in Fig. 5 for multiple values of ξ.

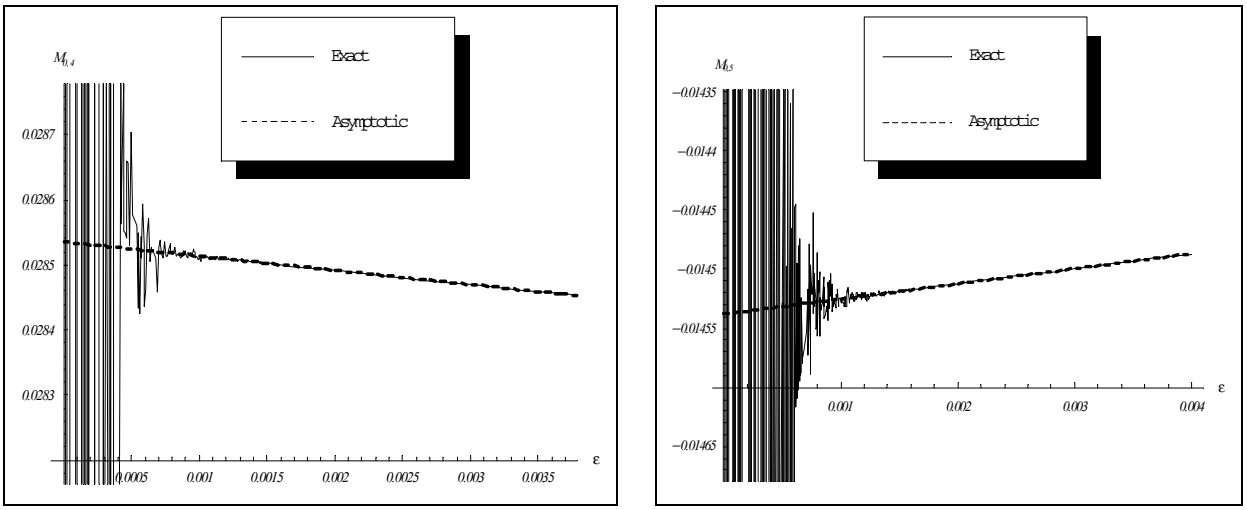

(a) $\xi = 20$ (b) $\xi = 50$

Figure 5. Exact and asymptotic expressions of the function $M_{0,l}$ of different orders versus the cell optical thickness

Now we turn our attention to the effect of the asymptotic analysis on the source multipliers. In this presentation, we identify the components of the source multipliers responsible for the instabilities in the spatial weights, and then plot these components using the full and the asymptotic expressions. For example, for the case ξ>1, the weights $S_{0,j,k}$ and $R_{i,0,k}$ will be investigated. For the case ξ<1, on the other hand, the weights $S_{i,0,k}$ and $R_{0,j,k}$ will be investigated.

In these plots we address the elimination of the oscillation as $\varepsilon \to 0$ and the agreement between the exact and asymptotic expressions far from the region where the oscillation occur in the exact expressions.

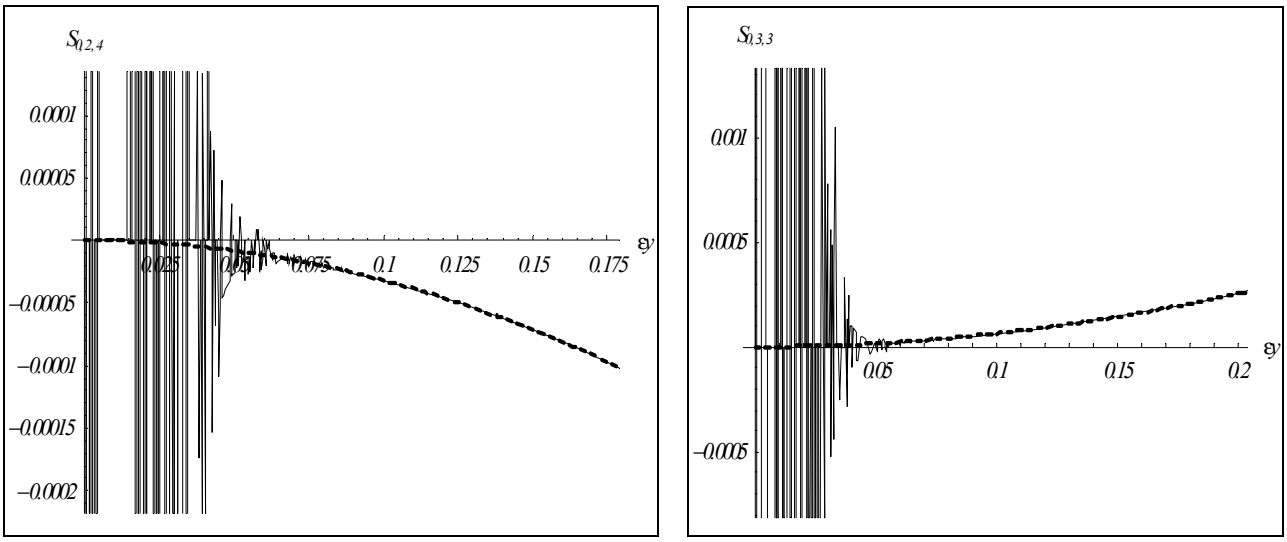

(a) (b)

Figure 6. Plot of the exact (solid line) and asymptotic (dashed line) expressions of the coefficient $S_{0,2,4}$ (a) and $S_{0,3,3}$ (b).

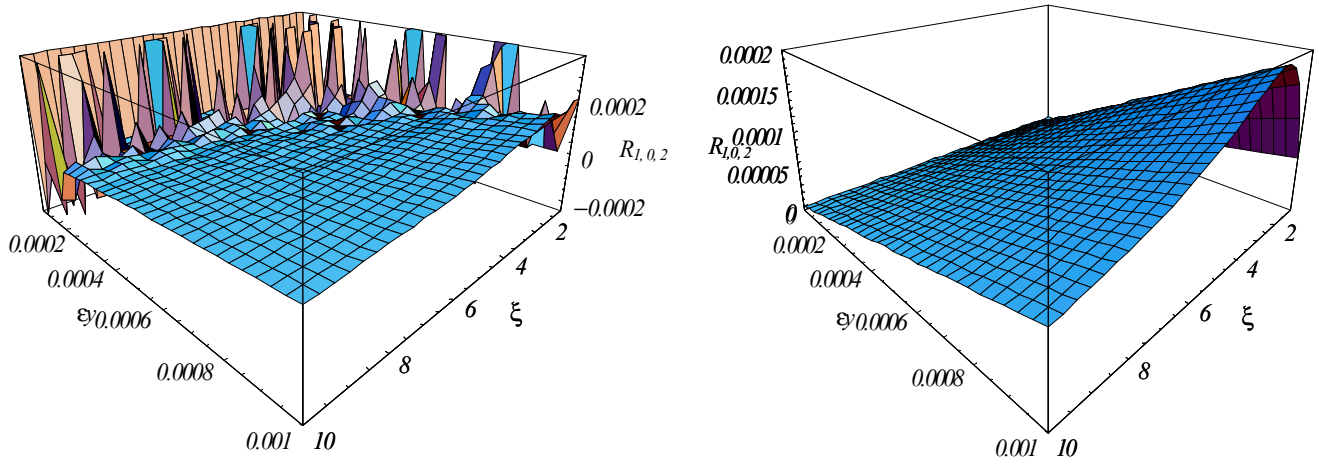

(a) (b)

Figure 7. Surface plots of the coefficient $R_{1,0,2}$ versus the cell optical thickness ε_y and the cell aspect ratio ξ before (a) and after (b) performing the asymptotic analysis

Fig. 6 and Fig. 7 show the importance and effectiveness of the asymptotic analysis of the spatial weights $S_{0,j,k}$ and $R_{i,0,k}$ for the cases with ξ>1. Oscillations in the exact expressions due to finite precision have been eliminated by the asymptotic analysis which results in smooth behavior of the weights.

Next we consider the asymptotic formulas for the cases where ξ<1. The coefficients of interest are $S_{i,0,k}$ and $R_{0,j,k}$. Fig. 8 shows some selected coefficients before and after performing the asymptotic analysis on them.

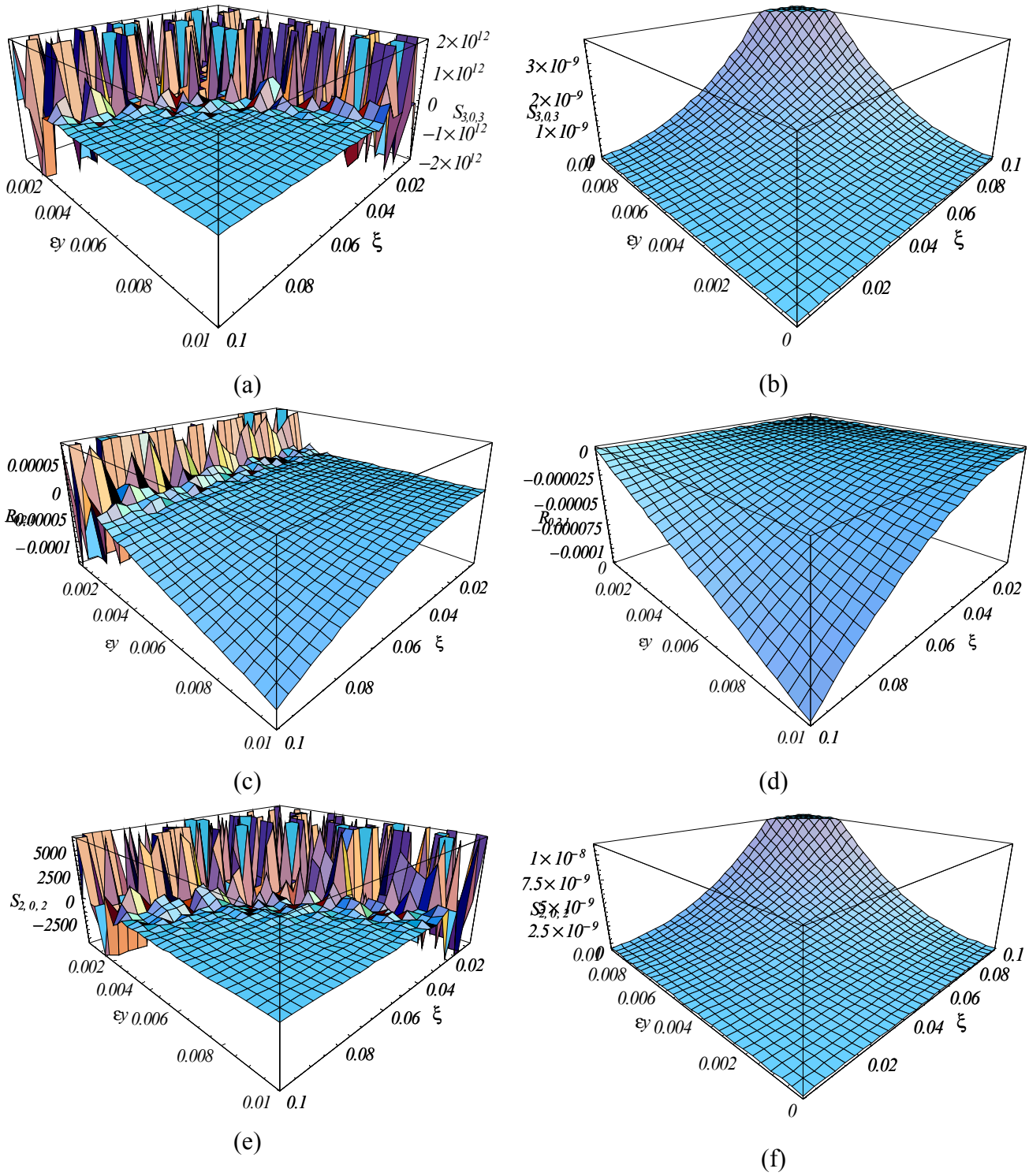

Figure 8. Surface plots of the coefficients $S_{3,0,3}$ before (a) and after (b) asymptotic analysis (for $\mu>0$ and $\eta<0$), $R_{0,2,1}$ before (c) and after (d) asymptotic analysis (for $\mu>0$ and $\eta<0$), and $S_{2,0,2}$ before (e) and after (f) asymptotic analysis (for $\mu<0$ and $\eta<0$).

5. CONCLUSIONS

We performed thin cell limit (asymptotic) analysis on the spatial weights of the Arbitrarily High Order Transport method of the Characteristic type (AHOT-C). We identified the components of the spatial weights responsible for the instabilities of the method, and then we expanded those components in truncated power series of the cell optical thickness. The derived formulas have worked fine for most of the cases that involved very thin cells and high orders.

In addition to performing thin cell analysis on the spatial weights, we have also derived new formulas for calculating the weights on thick cells. The new formulas performed as well as the old non-recursive formulas with the advantage of allowing performing thin cell analysis. Our new treatment of the spatial weights has been implemented in a research computer code developed at Oak Ridge National Laboratory to test the AHOT-C concept. Our implementation of the new analytic expressions of the weights has been successful so far and the code can run most of the cases that it could not run before.

As part of this research effort we have investigate the accuracy of the derived coefficients by running some difficult benchmark problems and comparing their results to those obtained with the AHOT-C code that uses the new asymptotic formulas. The benchmark results will be published in the near future.

REFERENCES

1. Azmy, Y. Y., "The Weighted Diamond-Difference Form of Nodal Transport Methods," *Nucl. Sci. Eng.*, **98**, pp. 29-40 (1988).
2. Azmy, Y. Y., "Arbitrarily High Order Characteristic Methods for Solving the Neutron Transport Equation," *Ann. Nucl. Energy*, **19**, No. 10-12, pp. 593-606, 1992.
3. Azmy, Y. Y., Zamonsky, O. M., "Thin-Cell Limit for the Spatial Weights of the Arbitrarily High Order Transport-Nodal Method," *Trans. Am. Nucl. Soc.*, **78**, pp. 130-132, 1998.
4. Elsawi, M. A., "*Asymptotic Analysis of the Spatial Weights of the Arbitrarily High Order Transport Method,*" Ph.D. dissertation. The University of Texas at Austin, 2001.